

Supplementary information

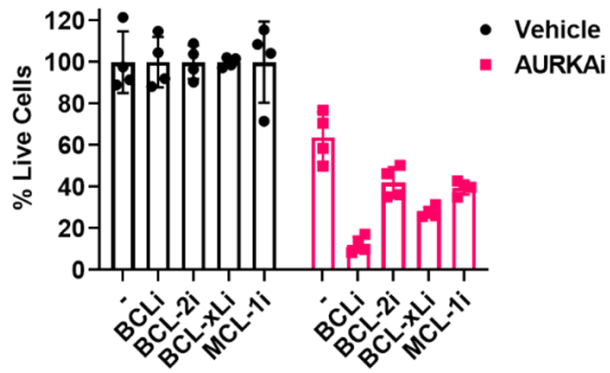
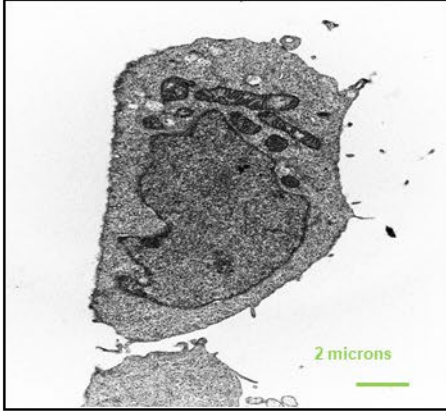


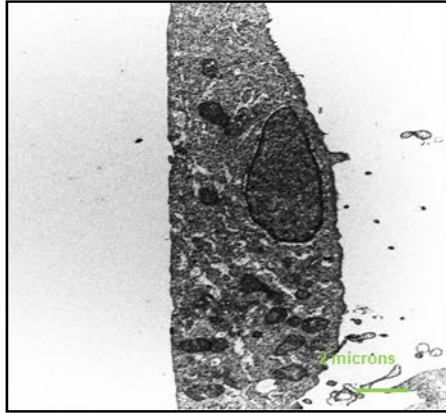
Figure S1. Inhibitors of BCL-2 family proteins promote melanoma cell response to AURKAI, Related to Figure 1. Relative cell numbers from the experiment are shown in Fig. 1K. Data are presented in percentages relative to cells treated with corresponding single-agent BCL-2 family inhibitor.

A**Cell morphology**

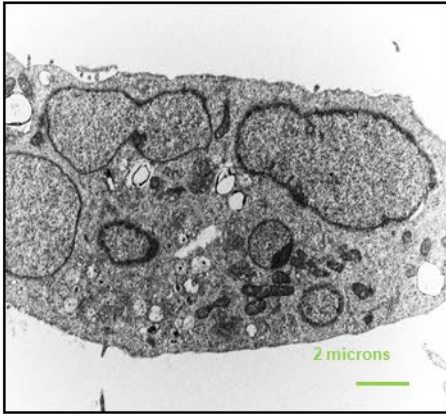
Vehicle



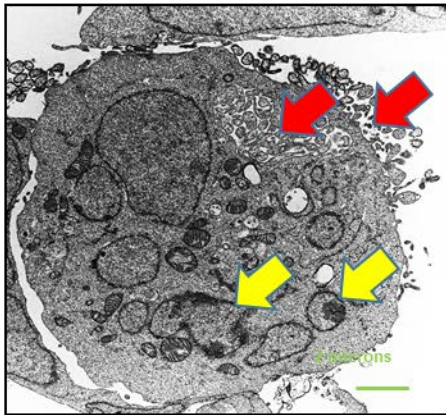
BCLI



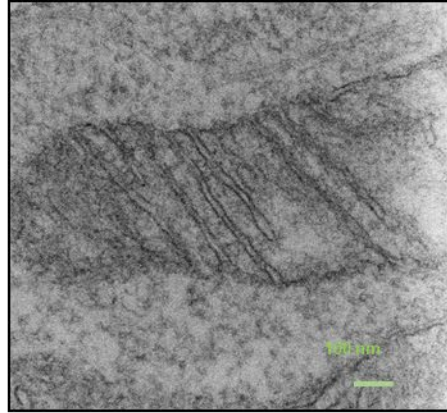
AURKAI



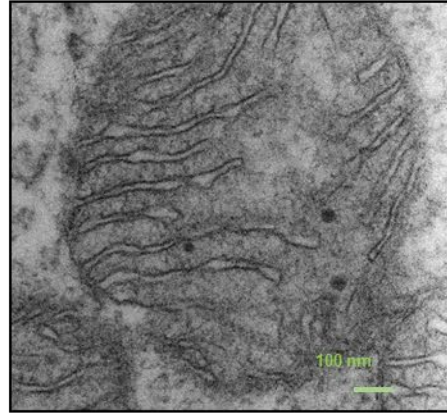
Combo

**B****Mitochondrial morphology**

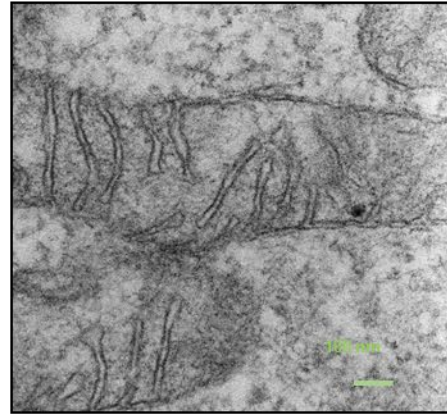
Vehicle



BCLI



AURKAI



Combo

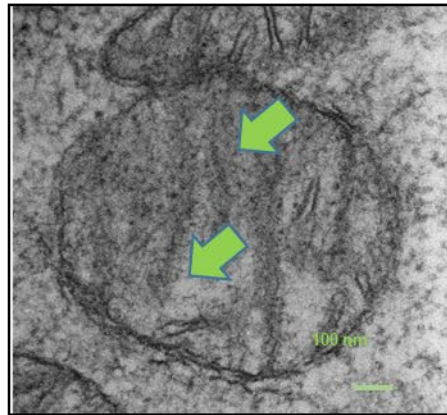


Figure S2. Cells treated with AURK_{Ai} and BCL_i combination display morphological hallmarks of apoptosis Related to Figure 2. Transmission electron microscopy (TEM) images of A375 cells after 16-hour treatment with vehicle, navitoclax (BCL_i, 1 μ M), alisertib (AURK_{Ai}, 1 μ M), and Combo. **(A)** Overall cellular changes were obtained at 6500X magnification. Red and yellow arrows point out apoptotic bodies and chromatin condensation, respectively. **(B)** Images illustrating mitochondrial morphology were obtained at 11000X magnification. Green arrows point to abnormal mitochondrial morphology in AURK_{Ai}/BCL_i-treated cells, as evident by the fragmented and irregular tubular and lamellar structure of cristae. Seven to eight random field images were taken from 2 slides per experimental condition.

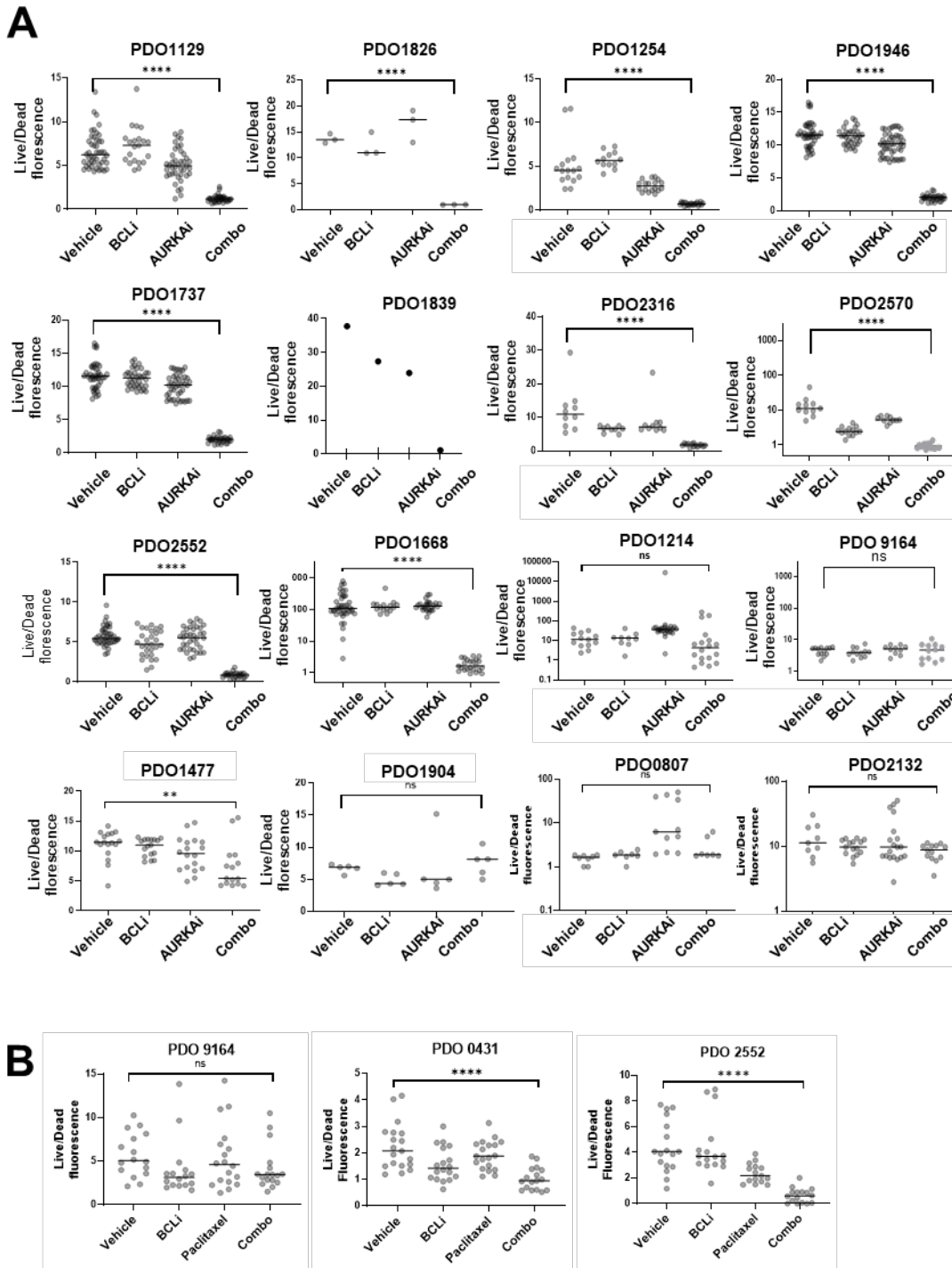


Figure S3. Combining BCLi with AURKAI or paclitaxel induces cell death in most melanoma PDOs, Related to Figure 3. (A) Comparisons of the live/dead (green/red) fluorescent signal ratios in individual PDOs treated with vehicle, 1 μ M navitoclax (BCLi), 1 μ M alisertib (AURKAI) or both drugs combined for 72hrs. Cells were incubated with calcein-AM (live cells), propidium iodide (PI, dead cells), and Hoechst 33342 (DNA dye) before imaging. The total number of organoids quantified in each treatment condition ranged from 1 to 40. Each dot on the plot represents an individual organoid. Horizontal lines on plots represent the median. Statistical comparison was performed using one-way ANOVA with Tukey's post-test. P-values were adjusted for multiple comparisons. Ns $P > 0.05$, * $P \leq 0.05$, ** $P \leq 0.01$, *** $P \leq 0.001$, **** $P \leq 0.0001$. No statistical analysis was performed for PDO 1839. (B) Same as A, except organoids were treated with vehicle, 1 μ M navitoclax (BCLi), 1 μ M paclitaxel, or both drugs combined for 72hrs.

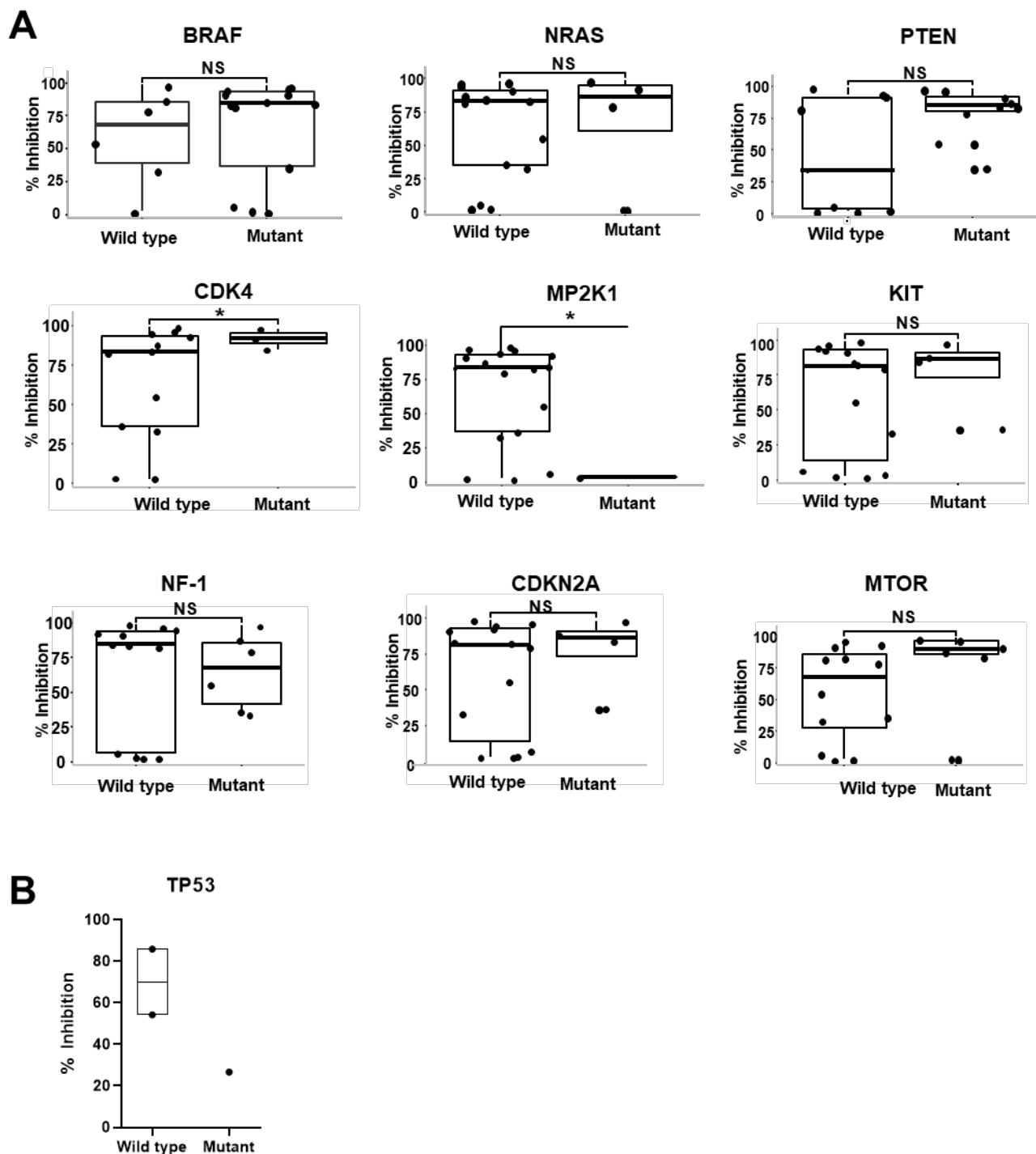


Figure S4. Association of AURKAI and BCLi response with genetic alterations in PDOs, Related to Figure 3. (A) Genetic alterations in PDOs were determined using targeted DNA sequencing. Response to alisertib/navitoclax combination was defined as a fold reduction of an average green/red (live/dead) ratio in PDOs after alisertib/navitoclax combination treatment compared to vehicle treatment. The correlation was queried using a two-sample t-test. Dunnett's method was used to adjust for multiple comparisons. (B) Association of TP53 mutational status with PDO responsiveness to treatment with navitoclax (1 μ M) and paclitaxel (0.1 μ M) combination for 72 hours. The % inhibition was calculated as described in A.

Figure S5. AURKai and BCLi combination treatment activated caspase 3 in tumor cells but had minimal effect on bone marrow cells and non-malignant human fibroblasts, Related to Figure 4. (A) Representative images of B16F10 tumor processed for activated caspase-3 (cleaved cas-3) immunofluorescence (IF) staining after 11 days of drug treatment. The right panel showed quantified images (n=4-11). 1-way ANOVA used for Statistical analysis. Treatment effects compared to vehicle control were analyzed using Dunnett's multiple comparisons test. Scale bar =150 μ M (B) Spectral cytometry analysis of bone marrow cells from mice is shown in Fig. 4A. Scatter plots showing the distribution of bone marrow cells across UMAP dimensions built based on the 23-immune marker expression data. Color represents the relative expression of a given marker (indicated to the right of the plots) in plotted cells. Deep red color marks cells with the highest marker expression, and dark blue color marks cells with the lowest marker expression. UMAP plots were constructed as described in Fig. 4G, H. (C) Representative images of crystal violet-stained patient-derived fibroblast cells treated with vehicle, 1 μ M navitoclax (BCLi), 1 μ M alisertib (AURKai), or both drugs combined for 24 h. The scale bar is 275 μ m. (D) Data quantification (n=3 biological replicates) and statistical analysis using 1-way ANOVA with Dunnett's multiple comparisons test. Ns P > 0.05.

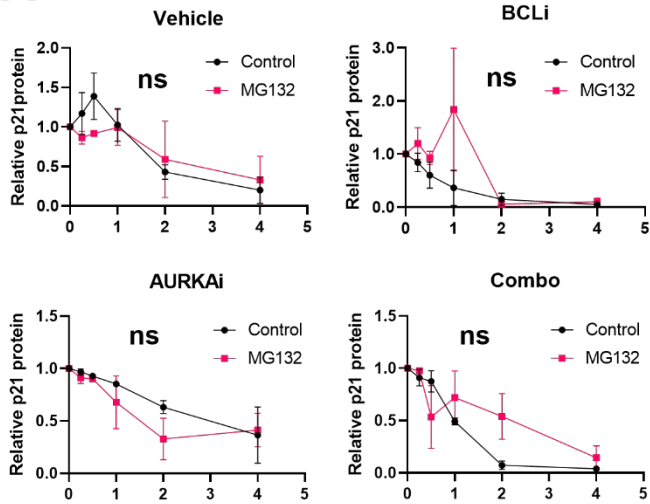
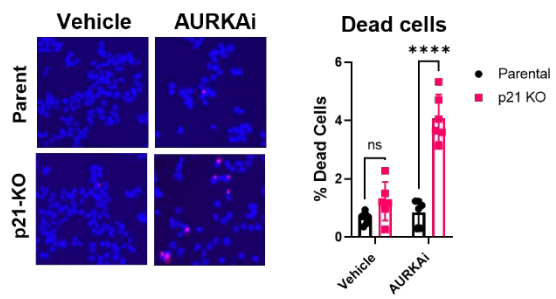
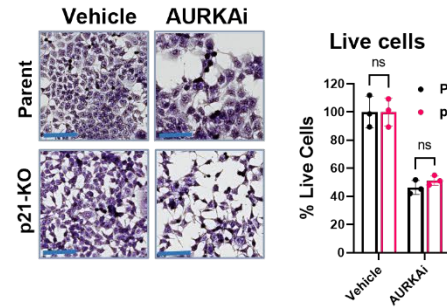
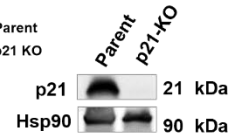
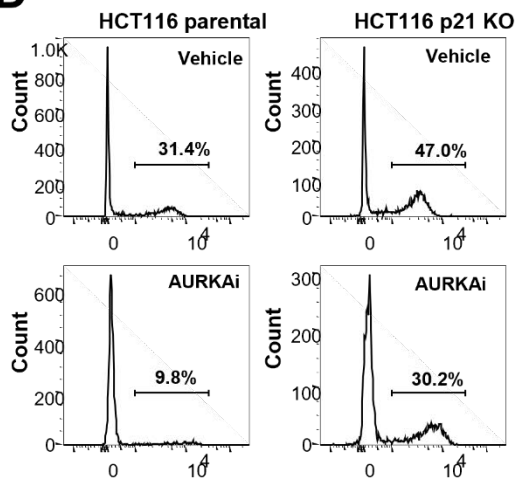
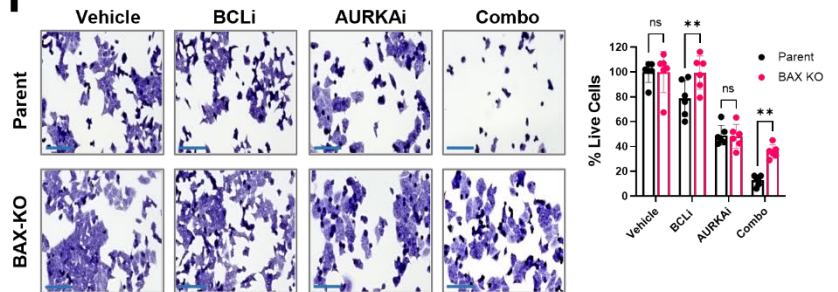
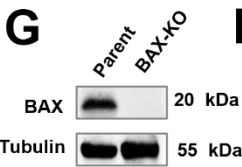
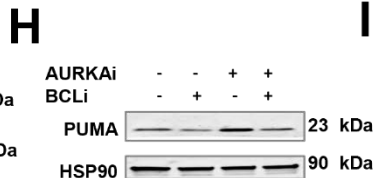
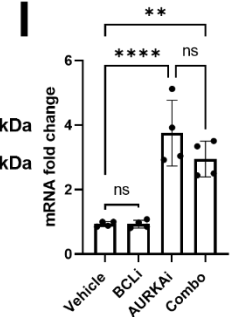
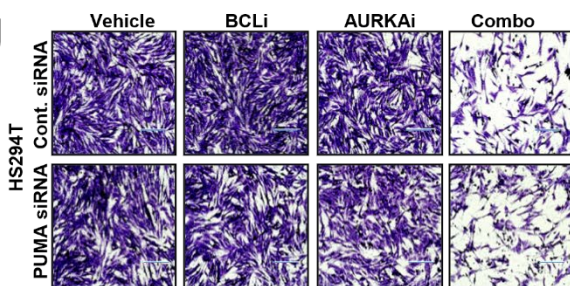
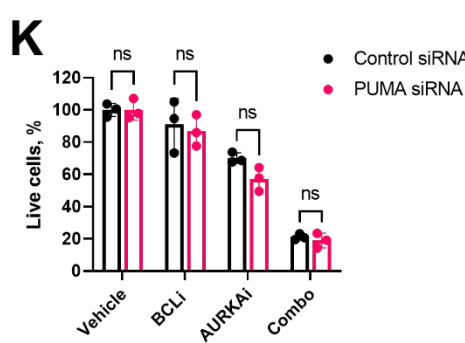
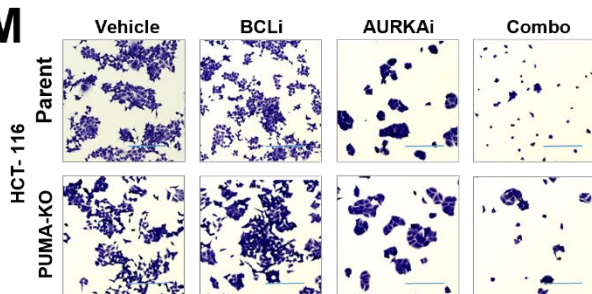
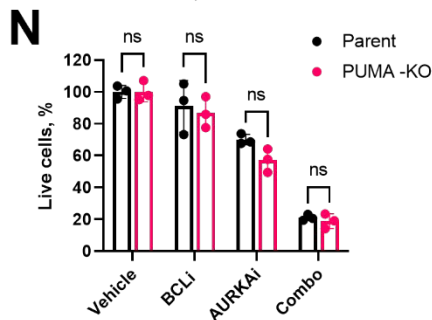
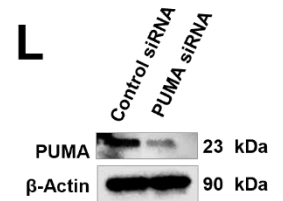
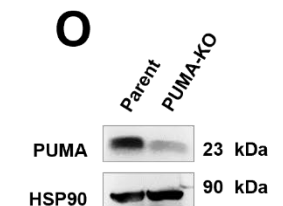
A**B****C****E****D****F****G****H****I****J****K****M****N****L****O**

Figure S6. P53 target genes regulate cellular responses to AURKAI and BCLi treatment, Related to Figure 7. (A) Analysis of p21 degradation in the presence and absence of proteasome inhibitor MG132. A375 melanoma cells were treated with vehicle, 1 μ M navitoclax (BCLi), 1 μ M alisertib (AURKAI), or a combination of both drugs for 16hrs followed by the addition of protein synthesis inhibitor Cycloheximide (150 μ g/ml). Data are pulled from two independent experiments. A representative experiment is shown in Fig. 7C. P21 expression was quantified using densitometry and normalized to the densitometry values for the corresponding actin band. The square root transformation was used to correct for heteroscedasticity. Statistical analysis was performed using 2-way ANOVA. (B) Representative images of HCT-116 wild-type (parent) and p21 knockout (p21-KO) cells treated with vehicle or 1 μ M alisertib (AURKAI) for 24 hrs and stained with Hoechst and PI. Scale bar 150 μ m. The right panel shows data quantification (n=6) and statistical analysis using 2-way ANOVA with Sidak's multiple comparisons test. (C) Same as B, except cells were stained with crystal violet and counted. N=3. (D) Analysis of BrdU incorporation by parental and p21 KO HCT116 cells after 72h treatment with 1 μ M AURKAI or vehicle. Percentages of BRDU+ cells are indicated on the plots. (E) Western blot analysis of p21 expression in HCT-116 parental and p21 KO cells. (F) Representative images and quantification of crystal violet-stained HCT-116 cells with and without the knockout of BAX. HCT116 cells were treated as in A. Scale bar 150 μ m. Three independent experiments were performed with consistent results. Statistical comparison was performed using one-way ANOVA with Sidak's multiple comparisons test. N=6. (G) Western blot analysis of BAX protein expression in HCT-116 parental and HCT-116 BAX-knockout cells. (H) Western blot analysis of PUMA protein expression in A375 cells treated with vehicle, 1 μ M navitoclax (BCLi), 1 μ M alisertib (AURKAI) or their combination for 24 hrs. (I) Real-time PCR analysis of relative *BBC3* (PUMA gene) mRNA in A375 cells treated as in B. Three independent tests were done with consistent results. (J) Representative images of crystal violet-stained Hs294T cells transfected with non-targeting or *BBC3* (PUMA)-targeting siRNA. (K) Quantified cell numbers from the experiment shown in C. N=3 biological replicates. Statistical comparison was performed using one-way ANOVA with Sidak's multiple comparisons test. (L) Western blot analysis of PUMA expression in Hs294T cells (M) Representative images of crystal violet-stained HCT116 cells with and without the knockout of endogenous *BBC3* (PUMA) gene. Cells were treated with vehicle, navitoclax (1 μ M, BCLi), alisertib (1 μ M, AURKAI), or a combination for 24 hrs. Two independent experiments (three replicates each) were performed with consistent results. (N) Quantified crystal violet assay data from three biological replicates. Statistical comparison as in E. Ns - P > 0.05, * - P \leq 0.05, ** - P \leq 0.01, *** - P \leq 0.001, **** - P \leq 0.0001. P-values were adjusted for multiple comparisons. (O) Western blot analysis of knockout in HCT116 cells.

Supplementary tables:

Table S1 (Drug screen results, related to Figure 1) is submitted individually as an Excel spreadsheet.

Table S2. Associations of PDO response to AURKai and BCLi combination treatment and tumor mutational/copy number status, Related to Figure 3. Y – yes/present. N – no/not present. n/a – information not available.

PDX ID	Sex	% viability loss on AURKai and BCLi	Gene mutations										Copy number alterations					
			BRAF	NRAS	P53	NF1	CDKN2A	PTEN	MTOR	MAP2K1	KIT	CDK4	NRAS	KIT	PTEN	NF1	MTOR	CDK4
2552	M	85	V600E	N	N	N	Stop Lost	T398S	G580A N382S	N	G265S	I51V G45A G44A	n/a	n/a	n/a	n/a	n/a	n/a
1668	M	98	S147N N140T	N	N	Stop Lost	Stop Lost	T398S	T1837S G580A N382S	N	M541L	I51V G45A G44A	n/a	n/a	n/a	n/a	n/a	n/a
1826	M	92	V600E	N	N	N	N	T398S	T1837S G580A N382S	N	N	I51V G45A G44A	1.19	1.48	1.26	0.94	1.08	052
1179	n/a	99	N	Q61H	N	N	N	N	K1981E	N	N	N	1.79	n/a	1.30	1.30	3.00	1.14
1946	F	84	V600E	N	N	N	N	G129E	N	N	N	N	1.56	n/a	1.41	1.95	1.87	1.84
1737	M	95	BRAFc .1798 1799GT >AA	N	N	N	N	N	N	N	N	N	n/a	n/a	n/a	n/a	n/a	n/a
1839	F	97	V600E	N	N	N	N	Stop Lost	N	N	N	N	2.36	2.33	1.46	1.85	1.61	1.47
1129	F	83	D549N K483T	N	N	N	N	N	N	N	N	N	n/a	n/a	n/a	n/a	n/a	n/a
0431	F	56	N	N	N	y	N	y	N	N	N	N	0.89	14.4	0.59	0.71	4.35	1.56
2316	F	88	N	N	N	Stop Lost	Stop Lost	Y	T1837S G580A	N	M541L K642E	N	2.51	N	1.26	2.27	2.42	1.93
2570	F	93	N and V600E	N	N	N	N	N	N	N	N	N	n/a	n/a	n/a	n/a	n/a	n/a
1662	F	80	N	Q61R	N	Y	N	Y	N	N	N	n/a	n/a	n/a	n/a	n/a	n/a	n/a
1254	n/a	87	V600E	n/a	n/a	n/a	n/a	n/a	n/a	n/a	n/a	n/a	n/a	n/a	n/a	n/a	n/a	n/a
9164	n/a	03	V600E	N	Stop Lost	N	N	N	N	N	N	n/a	n/a	n/a	n/a	n/a	n/a	n/a
1904	M	07	V600E	N	Y	N	N	N	N	N	N	n/a	2.02	2.92	1.40	1.60	2.03	1.97
1477	F	34	N	N	Y	Y	N	N	N	N	N	N	2.02	2.91	1.41	1.61	1.97	1.14
2132	M	37	V600E	N	Y	Y	Y	Y	N	N	Y	N	1.94	N	1.58	1.56	2.10	1.54
1214	M	03	N	Q61L	Y	N	N	N	N	N	N	N	4.10	1.28	1.54	0.57	3.30	1.28
0807	F	04	P192Q	N	A138 ADG T140S	N	N	N	LR282L	D67N P124S	N	N	n/a	n/a	n/a	n/a	n/a	n/a

Table S3. Characterization of *TP53* mutations in melanoma PDOs, Related to Figure 3. ¹Data from raw data sequencing files. ²Data from www.CbioPortal.org. ³Data from OncoKB website. ⁴Data from COSMIC (Catalogue of Somatic Mutations in Cancer). ⁵Data from NCBI ClinVar website. ⁶The FATHMM-MKL value is the p-value used to predict the consequences of a particular mutation. Ranging from 0-1, values above 0.5 are deleterious, and those 0.7 and above are pathogenic. Values below 0.5 are neutral. **Abbreviations:** N/A= Not Applicable, Y= Yes, N= No, LOF= Loss of Function.

<u>PDX</u> ¹	<u>Somatic/ Germline</u> ¹	<u>Codon Change</u> ¹	<u>Amino Acid Change</u> ¹	<u>Domain Impacted</u> ²	<u>Hotspot (Y/N)</u> ²	<u>Mutation Type</u> ¹	<u>Mutational Effect</u> ²	<u>FATHMM-MKL Predication</u> ^{4,6}	<u>FATHMM-MKL Score</u> ^{4,6}	<u>OncoKB Prediction</u> ³	<u>ClinVar Prediction</u> ⁵
0807	N/A	N/A	A138ADG	DNA Binding	Y	Insertion	LOF	N/A	N/A	Likely Oncogenic	Unknown
0807	N/A	419 C>G	T140S	DNA Binding	N	Substitution	LOF	N/A	N/A	Likely Oncogenic	Unknown
0807	N/A	215 C>G	P72R	N/A	N	Polymorphism	N/A	Neutral	0.36	Unknown	Likely Benign
1214	Somatic	833 C>T	P278L	DNA Binding	Y	Substitution	LOF	Pathogenic	1.0	Likely Oncogenic	Conflicting Interpretations
1214	Germline	215 C>G	P72R	N/A	N	Polymorphism	N/A	Neutral	0.36	Unknown	Likely Benign
1477	Somatic	721 T>C	S241P	DNA Binding	Y	Substitution	LOF	Pathogenic	0.93	Likely Oncogenic	Uncertain Significance
1477	Germline	215 C>G	P72R	N/A	N	Polymorphism	N/A	Neutral	0.36	Unknown	Likely Benign
1904	Somatic	Deletion	LL264L	DNA Binding	Y	Deletion	LOF	N/A	N/A	Likely Oncogenic	Unknown
1904	Germline	215 C>G	P72R	N/A	N	Polymorphism	N/A	Neutral	0.36	Unknown	Likely Benign
2132	Somatic	960 G>C	K320N	Tetramer	N	Substitution	Unknown	Pathogenic	0.98	Unknown	Unknown
2132	Somatic	824 G>A	C275Y	DNA Binding	Y	Substitution	LOF	Pathogenic	1.0	Likely Oncogenic	Pathogenic/Likely Pathogenic
2132	Germline	215 C>G	P72R	N/A	N	Polymorphism	N/A	Neutral	0.36	Unknown	Likely Benign
9164	N/A	574 C>T	Q192*	DNA Binding	N	Stop Gained	LOF	Pathogenic	0.93	Likely Oncogenic	Pathogenic
9164	N/A	108 G>A	P36	Transactivation	N	Substitution	N/A	N/A	N/A	N/A	N/A